ACADEMIC PRESS

Available online at www.sciencedirect.com

SCIENCE DIRECT®

Journal of Magnetic Resonance 163 (2003) 99–104

JMR Journal of Magnetic Resonance

www.elsevier.com/locate/jmr

Hole-burning diffusion measurements in high magnetic field gradients

E.E. Sigmund* and W.P. Halperin

Northwestern University, Department of Physics and Astronomy, Evanston, IL 60208, USA

Received 5 December 2002; revised 8 April 2003

Abstract

We describe methods for the measurement of translational diffusion in very large static magnetic field gradients by NMR. The techniques use a "hole-burning" sequence that, with the use of fringe field gradients of 42 T/m, can image diffusion along one dimension on a submicron scale. Two varieties of this method are demonstrated, including a particularly efficient mode called the "hole–comb," in which multiple diffusion times comprising an entire diffusive evolution can be measured within the span of a single detected slice. The advantages and disadvantages of these methods are discussed, as well as their potential for addressing non-Fickian diffusion, diffusion in restricted media, and spatially inhomogeneous diffusion.

Keywords: NMR; Diffusion; Hole-burning; Fringe field

1. Introduction

Field-gradient NMR is a widespread research tool. The common ingredient to any of its applications is the labelling of space by the Larmor precession frequency of a nuclear species in the presence of a static magnetic field gradient $\vec{G}$:

$$\omega_0(z) = \gamma H_0(z) = \gamma \vec{G} \cdot \vec{r}. \quad (1)$$

Here γ is the gyromagnetic ratio of the nucleus, ω_0 is the Larmor frequency, and $\vec{r}$ is the position within the sample. Two applications of this spatial dependence are: (1) measurement of structure (imaging), and (2) measurement of motion (flow and diffusion). Diffusion measurements have been performed since the earliest days of NMR research [1–3] and are among the most widely used image contrast effects in magnetic resonance imaging (MRI) [4].

One particular area of interest has been performing NMR experiments in large field gradients. Recent work on three-dimensional NMR microimaging with applied gradients of 50 T/m have successfully achieved voxel volume resolution of 40 fl for biological cell imaging [5,6]. Another source of large gradients are those in the fringe fields of NMR magnets [7,8]. For common superconducting magnets, such gradients are often in the range of 50 T/m; for high-field resistive magnets ($H_0 \approx 30$ T) such as at the National High Magnetic Field Laboratory, fringe field gradients greater than 200 T/m exist. NMR superconducting magnet facilities with Maxwell pair design exist for the purpose of generating gradients of order 200 T/m [9]. Other gradient sources are those outside of devices designed to probe exterior material, such as the NMR-MOUSE [10], NMR well-logging tools [11,12], or the magnetic resonance force microscope [13]. Alternatively, the internal magnetic field gradients within materials with inhomogeneous magnetic susceptibility have been used to study porous structure [14,15]. A common issue to many of these cases is that the RF excitation pulses are "soft" and do not uniformly excite the sample, either due to spatial inhomogeneity in the H_1 field, the limited frequency bandwidth of a finite-duration pulse, or both. Recent studies have been performed to fully characterize the spin evolution in CPMG sequences of many "soft" pulses to correctly extract diffusive information [16,17]. Other analyses have been performed to adapt multiple-quantum coherence sequences to the field-gradient regime [18]. New techniques using "nutation echoes" formed through a combination of inhomogeneities in the static (H_0) and RF(H_1) fields have been developed

* Corresponding author. Fax: 1-312-926-5991.
E-mail address: esigmund@northwestern.edu (E.E. Sigmund).

1090-7807/03/$ - see front matter © 2003 Elsevier Science (USA). All rights reserved.
doi:10.1016/S1090-7807(03)00133-2

[19,20] and were included in a scheme showing the successful recovery of full chemical shift information in the presence of a static field gradient of 50 mT/m [21,22]. As these studies have shown, prospects and applications for field-gradient NMR capability are growing. Thus, it is essential to adapt existing NMR techniques to the field-gradient regime, as well as recognize capabilities that only large gradients provide.

In this article, we describe methods for the measurement of translational diffusion in large static field gradients in the fringe field of NMR magnets. These methods are of the "hole-burning" variety, in which long, low power RF pulses are used for spectrally (and thus spatially) selective irradiations prior to detection. The time evolution of such "holes" can be analyzed to extract diffusion information on a sub-micron scale. Such a selective excitation technique has been successfully applied in the past using internal magnetic field gradients to study porous structure with liquids [15] and using applied gradients to image the diffusion of gases [23,24]; the contrast of the present study with that work is in the geometry and spatial resolution of the resonant slice with a much larger magnitude of the applied gradient. In addition to providing a viable alternative to dephasing methods, the methods we describe have potential for spatially resolved study of non-standard diffusion processes.

2. Hole-burning diffusion sequences

Two hole-burning sequences are sketched in Fig. 1. The left panel shows a standard hole-burning sequence, employed in many NMR experiments as well as other spectroscopies [25–28]. Such an experiment consists of applying a long, low power pulse of length t_p to irradiate a narrow band in frequency, given by $\Delta\nu \approx 1/t_p$. In the presence of a static magnetic field gradient $\vec{G}$, such a pulse irradiates a narrow spatial hole perpendicular to the gradient direction. For example, in a gradient of $G = 42$ T/m, the thickness of a ^{1}H hole irradiated by a $t_p = 1$ ms pulse is approximately $\Delta z = \Delta\omega/\gamma G = 2\pi/\gamma G t_p \approx 0.6\,\mu$m. After a diffusion period τ has elapsed, a broad detection is performed of a large slice whose thickness is typically a few hundred μm. In this case, this takes the form of a Hahn echo sequence with "hard" RF pulses. If $\tau << T_1$, the spins irradiated with the burn pulse are "edited out," and do not appear in the broadly detected signal. As a function of the evolution time τ, the labelled spins diffuse, widening the hole shape while conserving its area (in the absence of relaxation). This time evolution can be analyzed to extract a diffusion coefficient. This technique works if the hole thickness can be made comparable to the diffusion length for an NMR experiment, which is typically a few μm for liquids. As mentioned above, fringe field gradients are sufficient for this purpose.

In the single-hole sequence, we must wait several spin–lattice relaxation times (T_1) after each acquisition for the magnetization to return to equilibrium. For long T_1, acquiring spectra at many values of the evolution time τ is time-consuming. A variation on the hole-burning sequence, sketched on the right in Fig. 1, circumvents this inconvenience by using more of the available detection slice. In this sequence, not one but a series of hole-burn excitation pulses are applied. They

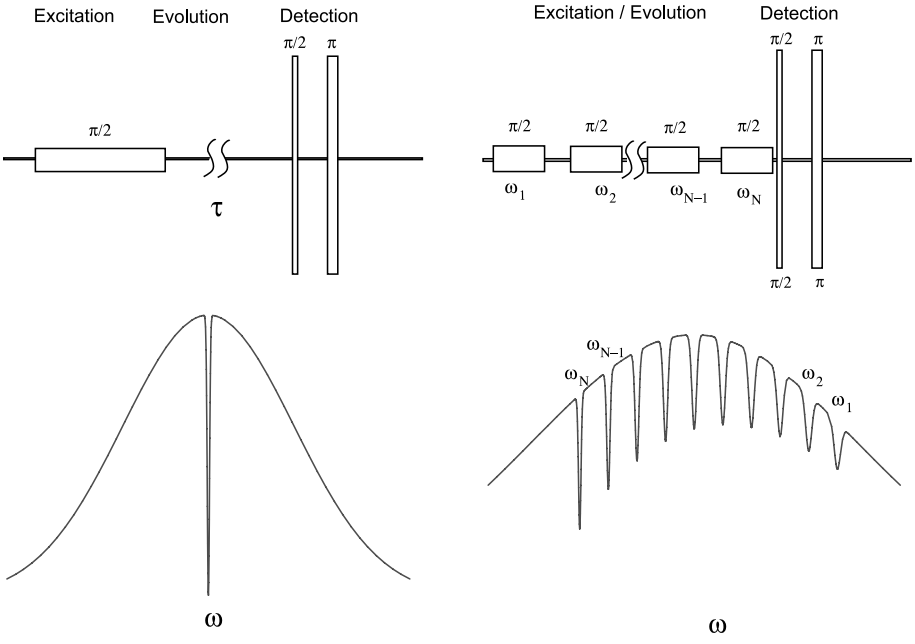

Fig. 1. Hole-burning diffusion sequences and sketches of spectral shapes. Left side: single hole-burning sequence. Right side: "hole–comb" sequence.

are spaced out in time on the scale of the diffusion time, and each is applied at a different frequency (i.e., position) within the bandwidth of the broad detection pulse. After this "hole–comb," the entire slice is detected, with the result sketched in the lower right panel of Fig. 1. The spins in the earlier holes diffuse while later holes are burned, so that the final spectrum contains a set of snapshots comprising an entire hole evolution. This technique assumes a uniform diffusion coefficient and field gradient across the slice, so all holes broaden at the same rate; for bulk liquids in fringe field gradients, this uniformity is excellent (within 0.1%). The evolution is acquired in a single transient; consequently, this sequence has a dramatically improved efficiency, and therefore provides higher sensitivity. The savings in acquisition time provides a signal-to-noise enhancement of $\sqrt{N}$, where N is the number of holes (or evolution times τ) in the sequence. We note that the hole–comb measurements we performed were made possible through the fast frequency switching capability of the MagRes2000 spectrometer designed by Reyes [29].

3. Analysis

In this section, we describe briefly the procedures used to extract a diffusion coefficient from a hole-burning experiment in a fixed field gradient. We denote the hole-burned absorption spectra at each evolution time τ as $F(\omega,\tau)$ and the unburned spectrum as $F_0(\omega)$. The first step is to define the hole shape from the larger slice shape

$$A(\omega,\tau) = 1 - \frac{F(\omega,\tau)}{F_0(\omega)}. \tag{2}$$

The hole shape $A(\omega,\tau)$ measures the profile of labelled spins along the gradient direction as a function of time. The hole's time evolution with time will be governed by the diffusive propagator $P(\omega,\tau;\omega',0)$. This gives the probability that a given spin at frequency ω' at time $t=0$ will be found at frequency ω at time $t=\tau$. For free, isotropic, diffusion, this 1-D propagator is well known

$$P(\omega,\tau;\omega',0) = \frac{1}{\gamma G\sqrt{4\pi D\tau}} \exp\left\{ -\frac{\left(\frac{\omega-\omega'}{\gamma G}\right)^2}{4D\tau} \right\}. \tag{3}$$

Given the propagator and the initial hole profile $A(\omega',0)$, the profile at a later time is found simply by the convolution product

$$A(\omega,\tau) = \int P(\omega,\tau;\omega',0)A(\omega',0)\,\mathrm{d}\omega'. \tag{4}$$

For example, we can calculate the explicit form of $A(\omega,\tau)$ for normal diffusion and a gaussian hole shape. Given a gaussian as an initial hole shape, i.e.,

$$A_g(\omega,0) = \exp\left\{ -\frac{\omega^2}{\sigma_0^2} \right\}. \tag{5}$$

Eq. (4) then becomes

$$A_g(\omega,\tau) = \frac{1}{\gamma G\sqrt{4\pi D\tau}} \int_{-\infty}^{\infty} \exp\left\{ -\frac{\left(\frac{\omega-\omega'}{\gamma G}\right)^2}{4D\tau} \right\} \times \exp\left\{ -\frac{\omega' 2}{\sigma_0^2} \right\} \mathrm{d}\omega'. \tag{6}$$

This gaussian integral can be easily performed by completing the square and using $\int_{-\infty}^{\infty} \exp(-ax^2)\,\mathrm{d}x = \sqrt{\pi/a}$. The result is

$$A_g(\omega,\tau) = \frac{\sigma_0}{\sigma(\tau)} \exp\left(-\frac{\omega^2}{\sigma^2(\tau)} \right), \tag{7}$$

where

$$\sigma^2(\tau) = \sigma_0^2 + 4\gamma^2 G^2 D\tau. \tag{8}$$

We see that this result conserves the area of the hole, as expected; the amplitude of the gaussian decays just as the width is enlarged. Once the initial width has been measured and fixed (through a spectrum measurement immediately following the burn pulse), all subsequent spectra can each be fit with a single adjustable parameter σ. The resulting square-widths can then be fit to linear time dependence to extract the diffusivity D. Thus far, in our experiments, we have used square-wave pulses which would be expected to burn sinc-function rather than gaussian holes. However, the gaussian is a convenient phenomenological form that, as shown in the experiments below, accurately describes the broadening of the hole.

The resolution limits of this mode of diffusion measurement are determined by the spin relaxation times, T_1 and T_2. Spin–lattice relaxation causes the tag placed on the burned spins to evaporate, and fills in the hole without broadening. In our measurements, we separately measure the spin–lattice relaxation time T_1 and constrain the hole area to decay as $\exp(-\tau/T_1)$. For sufficiently fast spin–lattice relaxation compared to the diffusion time, the hole broadening due to diffusion is undetectable. The minimum hole thickness is another bound on the experiment, determined either by the diffusivity D (fast limit), or by the spin–spin relaxation time T_2 (slow limit). The hole thickness is controllable only if negligible diffusion or spin dephasing takes place during the burn pulse length t_p. The combined conditions place the following lower bounds on measurable diffusivities by this method, depending on the controlling factor in the minimum hole size (diffusion or spin–spin relaxation) [30].

For diffusion-limited holes

$$\left(\frac{\gamma}{2\pi}\right)^2 G^2 D > \frac{1}{2}\frac{1}{T_1^3} \tag{9}$$

and for relaxation-limited holes

$$\left(\frac{\gamma}{2\pi}\right)^2 G^2 D > 2\frac{1}{T_1}\frac{1}{T_2^2}. \quad (10)$$

Eq. (10) is similar in form to the limiting diffusivity accessible from stimulated echo (STE) methods [9,30]. However, STE provides access to lower diffusivities than hole-burning, and with a much simpler analysis procedure. Hole-burning methods provide different advantages, as will be described later.

Given Eq. (10), an advantageous application of this method would be to a system with long T_2, such as was found, with ^{1}H decoupling, in the natural abundance ^{13}C signal in glassy glycerol in a previous NMR hole-burning study in a homogeneous field [28].

4. Experiment

Fig. 2 shows a measurement by a ^{1}H NMR hole-burning sequence of the diffusivity of propylene carbonate at $T = 295$ K. The corresponding individual hole shapes and their gaussian fits are shown in Fig. 3. The spin–lattice relaxation time T_1 in this case is of the order of seconds, much longer than the evolution times of the experiment (up to 30 ms). The resulting diffusivity is $D = (4.8 \pm 0.1)\ 10^{-6}\,\mathrm{cm}^2/\mathrm{s}$, which compares well with a diffusion measurement by a more standard stimulated echo dephasing measurement with the same sample and gradient.

Fig. 4 shows a measurement by a ^{1}H NMR hole–comb sequence of the diffusivity of glycerol-$^{13}C_2$ at $T = 296$ K. The corresponding individual hole shapes and their gaussian fits are shown in Fig. 5. In these fits, the area of the hole was constrained to decay as $\exp(-\tau/T_1)$, with a spin–lattice relaxation time of $T_1 = 112$ ms measured separately by a standard satura-

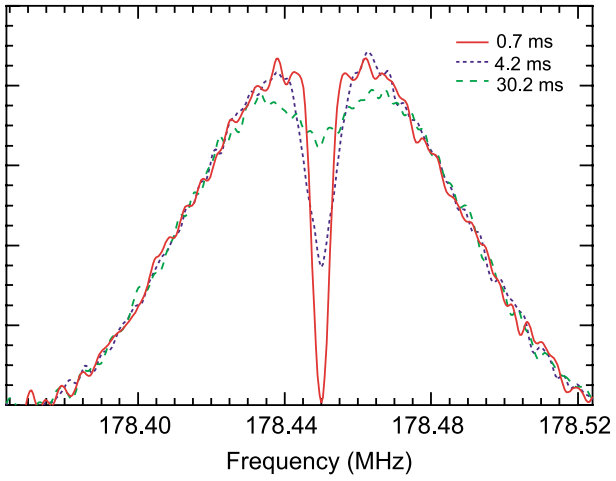

Fig. 2. Hole-burning diffusion measurement by ^{1}H NMR in propylene carbonate at $T = 295$ K in a gradient of $G = 42$ T/m.

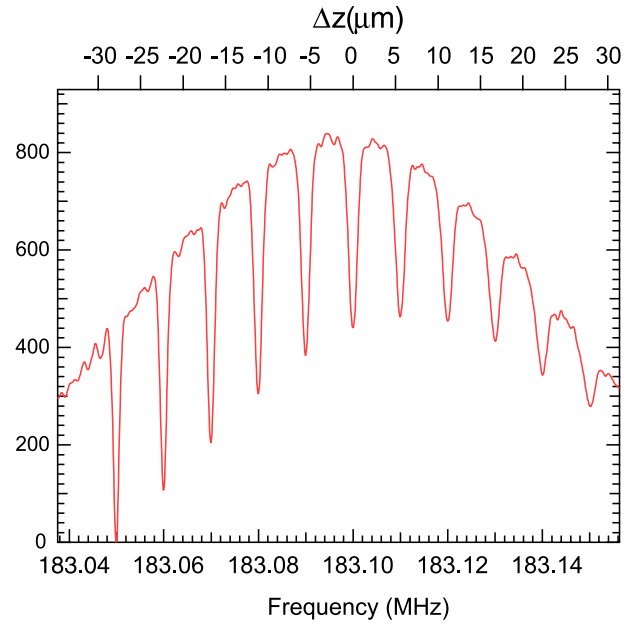

Fig. 4. Hole–comb diffusion measurement by ^{1}H NMR in glycerol at $T = 296$ K in a gradient of $G = 42$ T/m.

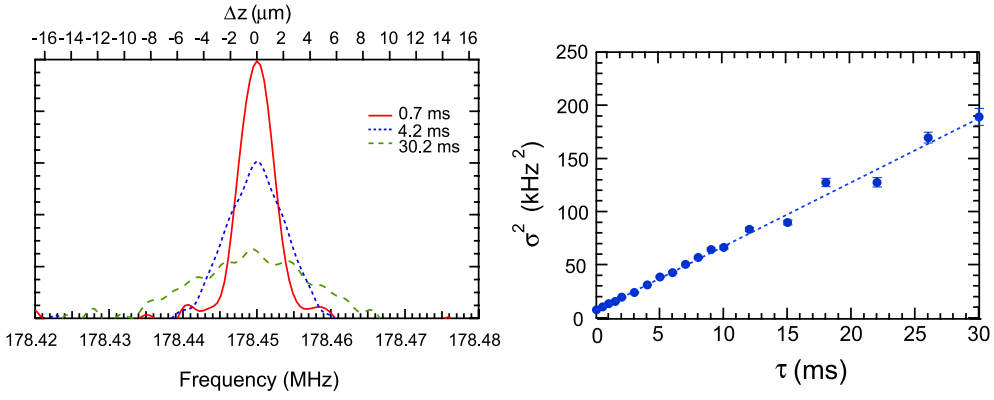

Fig. 3. Fits of hole-burning diffusion measurement by ^{1}H NMR in propylene carbonate at $T = 295$ K in a gradient of $G = 42$ T/m.

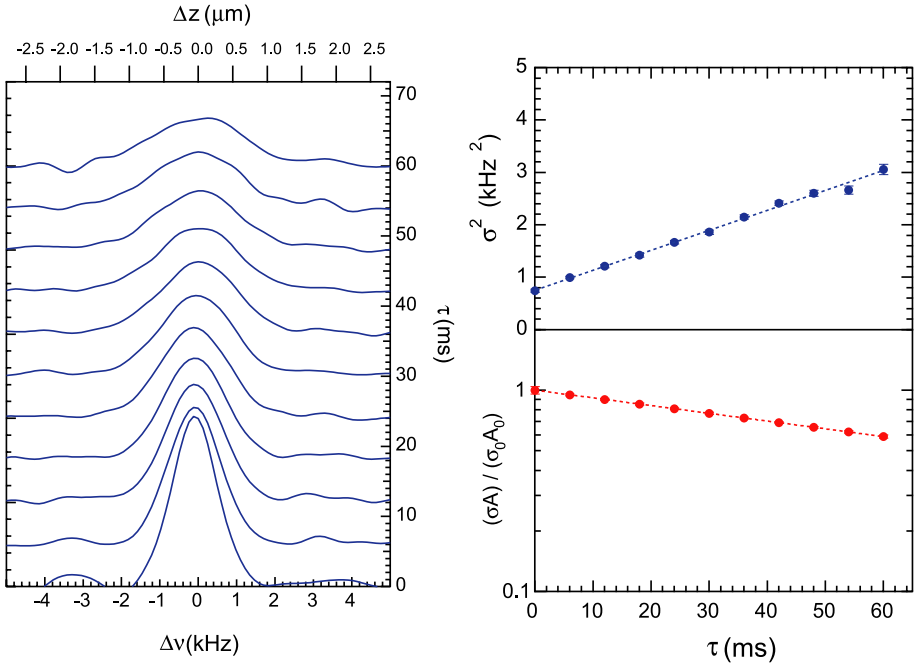

Fig. 5. Fits of hole–comb diffusion measurement by ^{1}H NMR in glycerol-$^{13}C_2$ at $T = 296$ K in a gradient of $G = 42$ T/m.

tion recovery sequence. The resulting diffusivity is $D = (2.86 \pm 0.05)\ 10^{-8}\,\mathrm{cm}^2/\mathrm{s}$, which again compares well with a stimulated echo diffusion measurement.

Finally, we show in Fig. 6 a comparison of temperature dependences of the glycerol-$^{13}C_2$ ^{1}H diffusion coefficient measured by two different methods: stimulated echo and hole–comb measurements. The agreement is good for higher temperatures, until the point that the burn pulse interval (≈1 ms) approaches the spin–spin relaxation time, T_2. At this point the hole–comb sequence becomes unreliable.

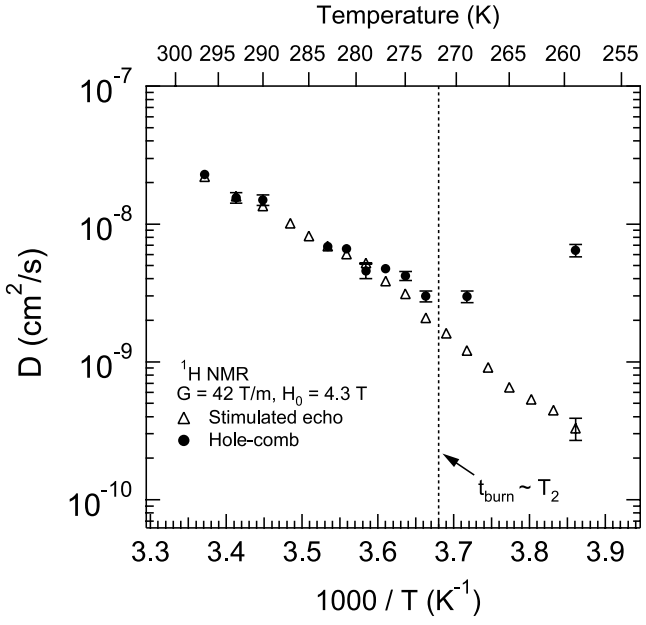

Fig. 6. ^{1}H NMR comparison of diffusivity measurements by stimulated echo and hole–comb techniques in the same sample of glycerol-$^{13}C_2$, with an applied gradient of $G = 42$ T/m. The two techniques agree until the spin–spin relaxation time T_2 is of order the burn pulse width t_{burn}; below this temperature translational diffusion cannot be correctly discerned by the hole–comb technique. The error bars are computed from the statistical accuracy of the fits, and are not shown if smaller than the symbol size.

5. Applications

For normal diffusion, a convenient form can be derived for the hole evolution given any initial hole shape. Alternatively, if the diffusive propagator is non-Fickian, this measurement can serve to map out its behavior by convoluting with a known excitation function. Given a spectral evolution profile from a hole-burning sequence, higher order moments can be calculated which provide more information on the propagator. Specifically, so long as the propagator is stationary, i.e. depends only on the difference of the observation times $\tau = t - t'$ and positions $Z = z - z'$, it can be shown that any spatial moment of an evolved hole spectrum $A(z,\tau)$, defined by

$$M_z^n[A(z,\tau)] \equiv \frac{\int \mathrm{d}z(z - \langle z\rangle)^n A(z,\tau)}{\int \mathrm{d}z A(z,\tau)} \tag{11}$$

is simply the sum of the initial hole moment and that of the diffusive propagator

$$M_z^n[A(z,\tau)] = M_z^n[A(z,0)] + M_Z^n[P(Z,\tau)]. \tag{12}$$

Thus, to the extent that any function can be reconstructed with knowledge of its moments, this provides a method for determining a non-Fickian propagator's

spatial dependence. The analogy with stimulated echo experiments (STE) is noteworthy [4]. In the hole-burning case, the Fourier transform of an echo transient is performed with respect to the readout gradient wavevector $k = \gamma G t$, while in the STE case an echo decay profile from multiple experiments is transformed with respect to $\vec{q} = \gamma G \tau_1$, where τ_1 is the interval between the first two pulses, to provide the propagator directly. The hole-burning sequence is potentially useful in the study of porous media, just as dephasing methods have been (e.g. [14,31]). If the initial hole size can be made less than the smallest confinement length scale, the crossover from free to restricted diffusion can be observed by steadily increasing the initial hole size. Such a variation is similar to that accomplished by variation of the first interval in a stimulated echo sequence. Finally, the spatial resolution of the hole-burning sequence is well-suited to problems of transport near surfaces; the diffusion coefficient in a liquid can be inspected on a submicron scale at arbitrary distances from a solid–liquid or solid–gas interface.

6. Conclusions

We have demonstrated a hole-burning NMR diffusometry technique in large magnetic field gradients ($G = 42\,\mathrm{T/m}$). This technique provides micron-scale resolution in one dimension for studies of normal and non-Fickian diffusion. Future directions include application to porous media and diffusion near surfaces on this scale.

Acknowledgments

We thank Y.-Q. Song and S. Lee for useful comments. This work has been supported by the NSF-MRSEC at the Materials Research Center at Northwestern University, Grant No. DMR-0076097.

References

[1] E.L. Hahn, Phys. Rev. 80 (1950) 580.
[2] H.Y. Carr, E.M. Purcell, Phys. Rev. 94 (1954) 630.
[3] S. Meiboom, D. Gill, Rev. Sci. Instrum. 29 (1958) 688.
[4] P. Callaghan, Principles of Nuclear Magnetic Resonance Microscopy, Oxford University Press, New York, 1991.
[5] D. Seeber, J. Hoftiezer, W. Daniel, M. Rutgers, C. Pennington, Rev. Sci. Instrum. 71 (2000).
[6] L. Ciobanu, D.A. Seeber, C.H. Pennington, J. Magn. Reson. 158 (2002) 178.
[7] R. Kimmich, W. Unrath, G. Schnur, E. Rommel, J. Magn. Reson. 91 (1991) 136.
[8] E.E. Sigmund, W.P. Halperin, R.E.A. Dillon, D.F. Shriver, Phys. Rev. B 64 (2001) 214201.
[9] B. Geil, Conc. Magn. Reson. 10 (1998) 299.
[10] G. Eidmann, R. Savelsberg, P. Blumler, B. Blümich, J. Magn. Reson. A 121 (1996) 104.
[11] R.L. Kleinberg, A. Sezginer, D.D. Griffin, M. Fukuhara, J. Magn. Reson. 97 (1992) 466.
[12] G. Goelman, M.G. Prammer, J. Magn. Reson. A 113 (1995) 11.
[13] A. Suter, D.V. Pelekhov, M.L. Roukes, P.C. Hammel, J. Magn. Reson. 154 (2002) 210.
[14] Y.-Q. Song, S. Ryu, P.N. Sen, Nature 406 (2000) 178.
[15] Y.-Q. Song, Phys. Rev. Lett. 85 (2000) 3878.
[16] M.D. Hürlimann, L. Venkataramanan, J. Magn. Reson. 157 (2002) 31.
[17] Y.-Q. Song, J. Magn. Reson. 157 (2002) 82.
[18] A. Wiesmath, C. Filip, D.E. Demco, B. Blümich, J. Magn. Reson. 154 (2002) 60.
[19] A. Jershow, Chem. Phys. Lett. 296 (1998) 466.
[20] A. Sharfenecker, I. Ardelean, R. Kimmich, J. Magn. Reson. 148 (2001) 363.
[21] C.A. Meriles, D. Sakellariou, H. Heise, A.J. Moulé, A. Pines, Science 293 (2001) 82.
[22] H. Heise, D. Sakellariou, C.A. Meriles, A. Moulé, A. Pines, J. Magn. Reson. 156 (2002) 146.
[23] M. Pfeffer, O. Lutz, J. Magn. Reson. 113 (1995) 108.
[24] I.E. Dimitrov, S.R. Charagundla, R. Rizi, R. Reddy, J.S. Leigh, Magn. Res. Imaging 17 (1999) 267.
[25] E.R. Hunt, J.R. Thompson, Phys. Rev. Lett. 20 (1968) 249.
[26] T.M. Duncan, A.M. Thayer, Phys. Rev. Lett. 63 (1989) 62.
[27] E.A. Hill, J.P. Yesinowski, J. Chem. Phys. 107 (1997) 346.
[28] P.L. Kuhns, M.S. Conradi, J. Chem. Phys. 77 (1982) 1771.
[29] A.P. Reyes, National High Magnetic Field Laboratory Annual Research Review, vol. 2000, 2001, p. 255.
[30] E.E. Sigmund, Ph.D. Thesis, Northwestern University, 2002.
[31] D. Topgaard, O. Söderman, Magn. Reson. Imaging 21 (2003) 69.